Indian Journal of Chemical Technology
Vol. 32, September 2025, pp. 572-583
DOI: 10.56042/ijct.v32i5.22518

Efficacy of hazardous congo red removal from aqueous solutions via adsorption with carbon black: Batch and column study insights

Saurabh Meshram[1], Nikhil Rahul Dhongde[2]*, Lucky Pandey[1], Gautam P Dewangan[1] & Anuradha N Joshi[1]

[1]Department of Chemical Engineering, Guru Ghasidas Vishwavidyalaya Bilaspur, Chhattisgarh-495 009, India

[2]Department of Chemistry, University of Saskatchewan, Saskatoon, Saskatchewan S7N5C9, Canada

*E-mail ID: nikhildhongde9194@gmail.com / nikhil.rahul@usask.ca

Received 8 August 2025; accepted 27 August 2025

This study investigates the potential of commercial carbon black, sourced from a local waste tyre recycling plant, as an adsorbent in both batch and continuous column adsorption processes for the removal of Congo red (CR). The carbon black has been characterized using Fourier transform infrared spectroscopy and scanning electron microscopy to assess its surface properties. Additionally, the study aims to analyze the physicochemical interactions between carbon black and CR. Key experimental variables, including adsorbent dosage, pH, and contact time, are optimized through batch adsorption experiments to determine their impact on the removal efficiency of CR dye. Batch adsorption experiments confirmed that carbon black (adsorbent) attains maximum adsorption capacities of 76.92 mg/g for CR dye. Among the tested kinetic models, the pseudo-second-order model (R^2 = 0.998) best described CR adsorption onto carbon black, outperforming the pseudo-first-order model (R^2 = 0.986). A continuous adsorption study has been done to determine the effect of the flow rate of water, adsorbent bed diameter and bed height on the breakthrough time. About 90% removal of CR occurs when the bed height is larger than 5 cm and the bed diameter is larger than 2.7 cm.

Keywords: Adsorption, Carbon black, Column Adsorption, Congo red, Dye removal, Wastewater

Introduction

As of 2025, the rapid industrialization and urbanization in India and the world have significantly exacerbated the water crisis, making it a critical issue for both sustainable development and public health[1–3]. Among the various industries contributing to water pollution, the textile industry stands out as one of the largest polluters, primarily due to its substantial consumption of water and the generation of large volumes of highly contaminated, coloured wastewater[4–6]. The dyeing and finishing processes in textile production, which involve the use of synthetic colourants, chemicals, and heavy metals, result in the discharge of effluents that are not only rich in hazardous substances but also persistently stained with synthetic dyes, causing severe contamination of water bodies[7–9]. The effluent's high organic load, combined with the toxic and non-biodegradable nature of many textile dyes, exacerbates the environmental impact, further straining the already dwindling water resources, specifically in India[10]. Effective management and treatment of these effluents have thus become crucial for mitigating the detrimental effects on aquatic ecosystems and ensuring the sustainability of water resources[11,12].

Azo dyes (AD), including Congo Red (CR), represent a significant category of synthetic colourants widely utilized in textile production, chiefly because of their extensive colour range, fade resilience and minimal energy requirements[13]. The azo bond, distinguished by its π-conjugation and resonance, confers remarkable stability to these dyes, rendering them resistant to photo degradation and adverse conditions[14]. This intrinsic stability is advantageous across multiple sectors, including textiles, paper, cosmetics, and pharmaceuticals. The extensive application of AD produces considerable wastewater laden with dye contaminants, notably CR, which is recognized for its carcinogenic properties attributed to its aromatic amine configuration[7,13]. The inclusion of benzene and naphthalene rings in the CR molecule enhances its environmental persistence, making it resistant to standard biodegradation techniques[15]. Moreover, CR demonstrates exceptional optical, thermal, and physicochemical stability, hence enhancing its environmental durability[16]. The release of wastewater containing CR into natural water bodies results in significant ecological repercussions, including the disturbance of aquatic ecosystems through elevated organic load, diminished light

penetration, and impaired photosynthesis. The poisonous, mutagenic, and carcinogenic properties of these dyes pose additional threats to aquatic organisms and human health, rendering the cleanup of CR contaminated water crucial for alleviating environmental and public health issues[17].

Diverse methodologies have been established for the elimination of dyes from wastewater, encompassing adsorption, membrane separation, flocculation and precipitation, and biodegradation[7,13,18]. Among them, adsorption has emerged as one of the most inexpensive, efficient, and uncomplicated ways of dye removal due to its simplicity, cost-effectiveness, and high removal efficacy [19,20]. Comprehensive studies have concentrated on improving adsorption efficiency by investigating low-cost, sustainable adsorbents sourced from accessible materials such as agricultural waste, fruit remnants, biomass, and industrial by-products. These alternative adsorbents provide a cost-effective option to traditional adsorbents while facilitating waste reduction and resource recovery, hence enhancing the sustainability of wastewater treatment systems.

Carbon black is a fine, black powder predominantly made of elemental carbon, generated during the incomplete combustion or pyrolysis of hydrocarbons, usually in an oxygen-limited environment[21–23]. Researchers have thoroughly investigated carbon black as an efficient adsorbent for the elimination of diverse pollutants from wastewater, encompassing organic substances such as phenol and inorganic contaminants like chlorine[24], mercury[15], chromium[25], etc. Carbon black, characterized by its extensive surface area, porous architecture, and many functional groups, offers a substantial quantity of active adsorption sites for the absorption of these pollutants[26].

Carbon black obtained from waste tires is generated via pyrolysis, a process in which end-of-life tires undergo thermal decomposition in an oxygen-free environment, resulting in a useful by product termed recovered carbon black[27]. This substance mitigates the environmental impact of non-biodegradable tyre trash and offers a sustainable substitute for virgin carbon black, conventionally derived from fossil fuels. Tyre-derived carbon black provides multiple advantages, such as less carbon emissions, economic efficiency, and the facilitation of a circular economy[28]. Its most intriguing attribute is its potential as an exceptional adsorbent, adept at eliminating contaminants from air, water, and industrial effluents owing to its extensive surface area and porous configuration[29]. At the local level, the establishment of recycling facilities for the recovery of carbon black from tires can stimulate green industry growth and reduce landfill use and open burning, serving as an effective mechanism for sustainable urban waste management.

To the best of the author's knowledge, while carbon black derived from local waste tyre recycling plants has been widely explored for wastewater treatment applications, there is a notable gap in the literature regarding its use for the removal of CR dye from aqueous solutions. Specifically, no studies have been found that investigate the adsorption of CR dye using carbon black through both batch and column studies. This research fills that gap by providing a comprehensive analysis of CR dye removal using carbon black in these two distinct experimental setups. This study investigates the removal of CR from aqueous solutions via adsorption onto carbon black. The carbon black adsorbent is meticulously examined by scanning electron microscopy (SEM) to analyze its surface shape and Fourier-transform infrared spectroscopy (FTIR) to ascertain functional groups. The impact of several parameters, such as pH, contact duration, and adsorbent dosage, on the adsorption capacity and removal efficiency of CR is systematically assessed via batch and column adsorption studies. This study presents an innovative method for utilising carbon black (from local waste tyre recycling plants) in dye elimination and offers significant data in the domain of wastewater treatment.

Experimental Section

Materials & reagents

Carbon black was procured from a local waste tyre recycling plant in Bilaspur, Chhattisgarh, India. CR was obtained from Bombay Glass and Chemical Works, Bilaspur, Chhattisgarh, India. A stock solution of 100 ppm was prepared and diluted to make 10, 20, 30, 40, and 50 ppm solutions for the determination of the calibration curve using a UV-VIS spectrophotometer (Shimadzu, Mumbai, India) at a wavelength of 497 nm.

For batch adsorption, 50 mL of water sample was added with a fixed amount of carbon black (adsorbent). The solution is then shaken for a predefined time in a shaker (Remi Mini, India) at a speed of 100 rpm. The solution passed through filter

paper (Whatman grade-1) to separate the adsorbent, and the residual concentration of CR was determined using a UV-Vis spectrophotometer at a wavelength of 497 nm. The effect of parameters pH (2, 4, 6, 8, 10), time (30, 60, 120, 150 and 180 min), and adsorbent dosage (0.2, 0.4, 0.6, 0.8 and 1 g/50 mL) is determined by varying one parameter while keeping other parameters constant. The pH of the solution was maintained by standard hydrochloric acid (0.1 M) and sodium hydroxide (0.1 M) solutions. To evaluate the performance of batch adsorption, the % removal of CR and adsorbent uptake (q_e) capacity are determined using Eq. (1) and Eq. (2), respectively[19,30,31].

$$\% \, Removal = \frac{(C_o - C_e)}{C_o} \times 100 \quad \ldots (1)$$

$$q_e = \frac{(C_o - C_e)V}{m} \quad \ldots (2)$$

Where C_o and C_e are the CR concentrations in the water at initial and equilibrium, respectively. V is the volume of the sample, and m is the mass of the adsorbent. For the continuous adsorption study, CR dye water (150 ppm) was prepared and allowed to flow through an adsorbent-filled column at a fixed flow rate. Columns of different diameters (1 cm, 2 cm, and 3 cm) and bed heights (2 cm, 4 cm, and 6 cm) were used to determine the effect on adsorption performance. The experimental run was determined using the Taguchi optimization method.

Characterisation

The surface morphology of the carbon black adsorbent was analyzed using a ZEISS EVO Series Scanning Electron Microscope Model. Before imaging, a gold (Au) sputter coating with a thickness of 0.5 to 1 nm was applied to the membrane samples using a Rotary Pumped Coater to improve surface impedance and assure excellent image quality during SEM analysis. The carbon black adsorbent was analyzed using FTIR spectroscopy (Bruker, Alpha Model) to investigate the chemical functional groups. The FTIR spectrum was recorded over the wavenumber range of 4000 to 500 cm^{-1}, which is typical for identifying a wide range of functional groups and structural features in organic and polymeric materials.

Results and Discussion

Characterization of carbon black adsorbent

The surface morphological characteristics of the adsorbent (carbon black) were evaluated through SEM analysis and shown in Fig. 1. The SEM images reveal that the carbon black forms fine, homogeneous agglomerates with a quasi-spherical shape[26,32]. Additionally, the surface features a smooth texture, characterized by a finer grain structure, which contributes to the overall homogeneity and potential adsorption capacity of the material. Chen *et al*.[33] and Dong *et al*.[34] also observed a similar trend in the SEM images of the carbon black adsorbent.

The surface functional groups present on carbon black were characterized using the FTIR spectroscopy as shown in Fig. 2. A prominent peak observed at 3819 cm^{-1} is likely to be associated with surface hydroxyl (OH) groups. The bands between 1300 and 1500 cm^{-1} are ascribed to the stretching vibrations of $–CH_2$ and $–CH_3$ groups. Additionally, the peak at 939 cm^{-1} indicates C–O stretching vibrations and bending modes of the O–H bond, typical of ether, lactone, and phenolic structures[26,32,35]. Finally, the

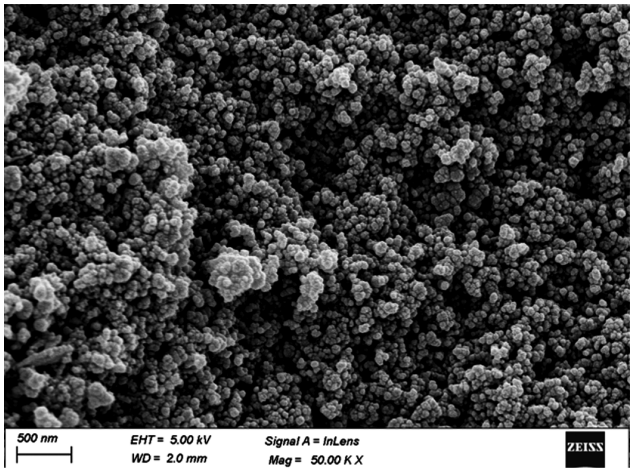

Fig. 1 — SEM micrograph of carbon black

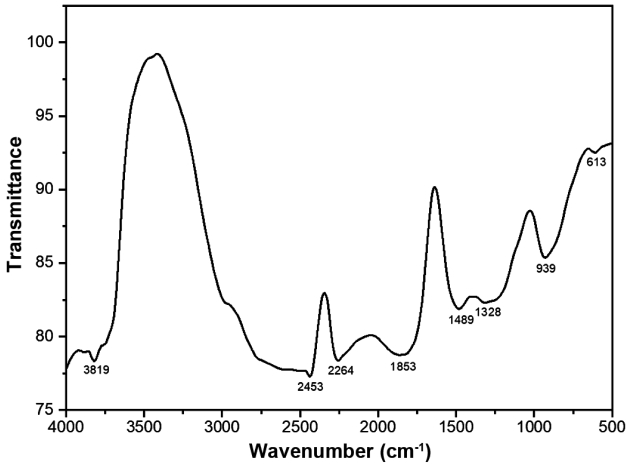

Fig. 2 — FTIR spectrum of carbon black

existence of C–C and C–H bonds is further confirmed by an additional peak at 613 cm^{-1}. These spectral features suggest a variety of oxygenated functional groups and hydrocarbons on the surface of carbon black[36,37].

Effect of different parameters on adsorption of CR dye

Effect of dose

The effect of the adsorbent dose on CR dye removal was investigated by varying the dose from 0.2 to 1 (g/50mL), while maintaining constant conditions of pH 2, contact time of 60 min, agitation speed of 100 rpm, and an initial dye concentration of 60 (mg/L). As shown in Fig. 3, the percentage of dye removal increases significantly with the adsorbent dose up to 0.6 (g/50mL), after which the increase in removal efficiency becomes minimal, even at higher doses up to 1 (g/50mL). This behaviour can be ascribed to the enhanced accessibility of adsorption sites, surface functional groups and an increase in the total surface area of the adsorbent, which promotes more efficient adsorption of CR ions[38]. At lower adsorbent dosages, the high concentration of CR ions around the adsorbent particles creates a steeper concentration gradient, facilitating enhanced dye adsorption[39]. However, beyond a certain point, the increase in adsorbent dose results in a lower increase in removal efficiency due to the point of adsorption site saturation and the limited capacity of the adsorbent. Therefore, by considering the optimum CR dye removal, further adsorption studies were performed at the carbon black dosage of 0.6 (mg/L).

Effect of pH

The effect of pH on the removal of CR dye was evaluated by varying the pH from 2 to 10 while keeping the other experimental parameters constant: contact time of 60 min, adsorbent dose of 0.6 (g/50mL), initial dye concentration of 60 (mg/L), and shaking speed of 100 rpm (Fig. 4). It was detected that the percentage removal of CR dye declined with an increase in pH. This behaviour can be attributed to two primary factors: (1) the electrostatic interaction between the protonated functional groups on the adsorbent surface and the anionic dye molecules, and (2) the chemical interactions between the dye and the adsorbent. At pH 2.0, the adsorbent surface is predominantly protonated, resulting in a surface with a positive charge that strongly attracts the negative-charged CR ions via electrostatic interactions,

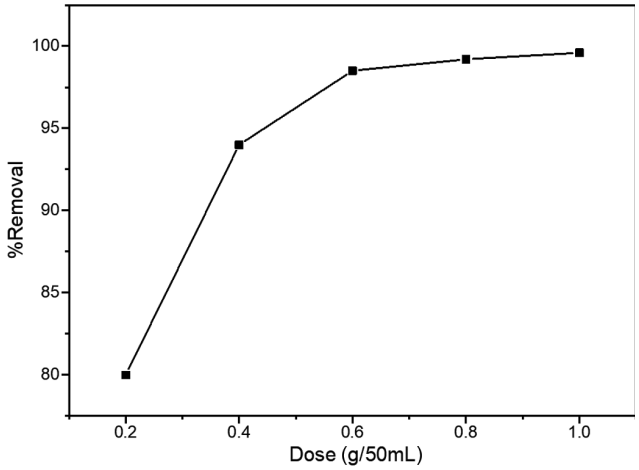

Fig. 3 — Effect of adsorbent dose on the removal of CR

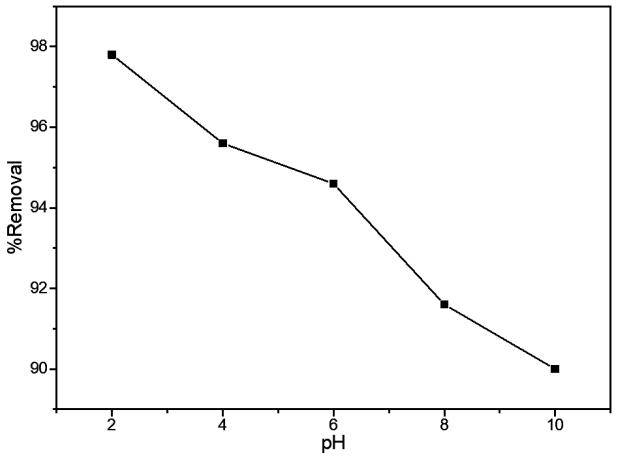

Fig. 4 — Effect of pH on removal of CR (time-60 min, dose-0.6 g/50 mL, speed-100 rpm, initial concentration-60 mg/L)

resulting in significant adsorption efficiency[40]. However, as the pH increases, the adsorbent's surface becomes more negatively charged due to the deprotonation of surface groups, which, in turn, reduces the electrostatic attraction between the adsorbent and the anionic dye[41]. At higher pH values, the increasing quantity of negatively charged spots on the adsorbent surface leads to electrostatic repulsion between the adsorbent and the negatively charged CR ions, thereby hindering the adsorption process and resulting in a reduced dye removal efficiency. At lower pH, the increased concentration of H^+ ions intensifies competition with CR ions for available adsorption sites on the carbon black adsorbent surface[42]. Additionally, the protonation of functional groups on the carbon black surface may lead to electrostatic repulsion of CR ions, hindering their adsorption onto the carbon black surface.

Additionally, at higher pH, the chemical interaction between the dye and the adsorbent may also be less favourable, further contributing to the decrease in adsorption[43].

Effect of time

The adsorption time was varied from 30 min to 180 min, with the parameters held constant at pH 2, agitation speed of 100 rpm, and an adsorbent dose of 0.6 g per 50 mL. Fig. 5 illustrates the impact of contact time on the percentage removal of CR dye. Initially, the removal rate is rapid, which can be attributed to the abundant availability of active sites on the surface of the adsorbent. During the early stages of adsorption, a significant number of adsorption sites are unoccupied, allowing for faster uptake of the dye. However, after the initial phase, between 30 and 90 min, the adsorption rate slows down. This deceleration is caused by increasing competition between the adsorbate molecules (CR) and the progressively occupied active sites on the adsorbent surface[10]. As the number of available sites decreases, the efficiency of adsorption diminishes, leading to a gradual reduction in the rate of removal.

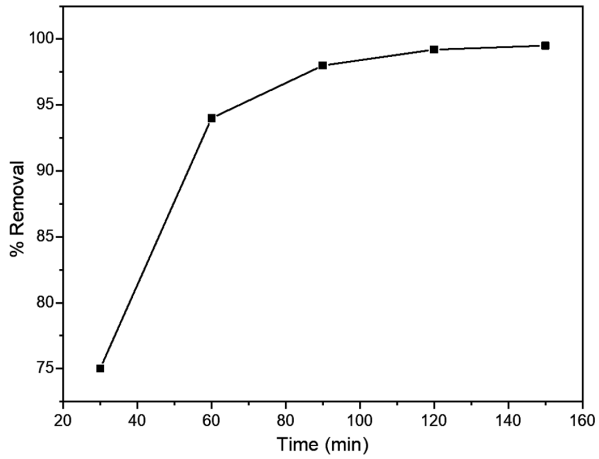

Fig. 5 — Effect of time on removal of CR (dose-0.6 g/50 mL, speed-100 rpm, initial concentration-60 mg/L, pH-2)

Isotherm study

Langmuir model

This model describes the monolayer adsorption process. The linear form of the equation for this model is given by Eq. (3).

$$\frac{C_e}{q_e} = \frac{1}{Q_0\, b} + \frac{C_e}{Q_0} \quad \ldots (3)$$

$$R_L = \frac{1}{1+bC_o} \quad \ldots (4)$$

where C_e represents the concentration of metal ions at equilibrium (mg/L), and q_e is the amount of adsorbate adsorbed per unit weight of adsorbent (mg/g). Q_o indicates the maximum adsorption capacity (mg/g), and b is a constant that represents the bonding energy.

Freundlich isotherm

The Freundlich isotherm model is used to describe the multilayer adsorption process and the heterogeneous characteristics of adsorption sites[25]. The empirical equation for the Freundlich isotherm is given by Eq. (5).

$$\log q_e = \log K_f + {}^{1}/_{n_f} \log C_e \quad \ldots (5)$$

In the Freundlich model, K_f and n represent the adsorption capacity and intensity, respectively. The values of K_f and n offer important insights into the heterogeneity and adsorption behaviour of the system. By plotting $\log(q_e)$ versus $\log(C_e)$, a linear relationship can be established, which allows for the determination of the model parameters K_f and $1/n$[19,30]. The regression coefficients and parameters for both the Langmuir and Freundlich isotherms are presented in Table 1. The results in Table 1 clearly indicate that the adsorption equilibrium data for the tested adsorbents fit the Langmuir isotherm model more closely than the Freundlich model, as evidenced by the higher R^2 values for the Langmuir model compared to the Freundlich model.

Table 1 — Langmuir and Freundlich, Dubinin-Radushkevich, and Temkin isotherm parameters for CR dye adsorption on carbon black at 308 K temperature

Isotherm parameters						
Langmuir Isotherm			Freundlich Isotherm		
q_m (mg/g)	K_L (L/mg)	R^2	1/n	K_F (mg/(g (mg/L)$^{1/n}$)	R^2
76.92	0.278	0.962	0.6114	3.406	0.999
Dubinin-Radushkevich (D-R) isotherm			Temkin Isotherm		
E (kJ/mol)	1/n	K_F mg/(g (mg/L)$^{1/n}$)	K_T (L/mg)	B_T (J/mol)	R^2
0.508	39.99	0.884	3.190	162.806	0.959

Dubinin-Radushkevich (D-R) isotherm

The Dubinin-Radushkevich (D-R) isotherm model distinguishes between chemical and physical adsorption processes. It is used to describe the Gaussian distribution of energy on the adsorbent surface[30]. The linear form of the D-R isotherm is expressed by Eq. (6), where ε represents the Polanyi potential, calculated using Eq. (7), R is the ideal gas constant, and T is the absolute temperature. The constant β is specific to the D-R model and is used to determine the mean free energy (E) of adsorption per adsorbate molecule, as given by Eq. (8).

$$\ln(q_e) = \ln(q_m) - \beta\varepsilon^2 \quad \ldots (6)$$

$$\varepsilon = RT \ln\left(1 + \frac{1}{C_e}\right) \quad \ldots (7)$$

$$E = 1 / \sqrt{2\beta} \quad \ldots (8)$$

Temkin isotherm

The Temkin isotherm model, on the other hand, assumes that the heat of adsorption decreases in a linear fashion with increasing surface coverage on the adsorbent. The linearized form of the Temkin isotherm model is represented as

$$qe = (RT/B_T) \ln K_T + (RT/B_T) \ln C_e \quad \ldots (9)$$

Where, B_T is the Temkin constant, which reflects the heat of adsorption, and K_T is the equilibrium binding constant associated with the maximum binding energy.

Plot of Langmuir, Freundlich, Dubinin-Radushkevich, and Temkin isotherms for the adsorption of CR onto carbon black are given Fig. 6. The adsorption capacity, as indicated by the correlation coefficient (R^2), is higher for the Freundlich isotherm (0.999) compared to the Langmuir isotherm (0.962). The Freundlich isotherm is better suited for systems with heterogeneous surfaces, where adsorption energy varies across the surface. In such cases, the adsorbate molecules interact with various sites on the adsorbent, leading to a higher overall adsorption capacity. This is because the Freundlich model accounts for the varying

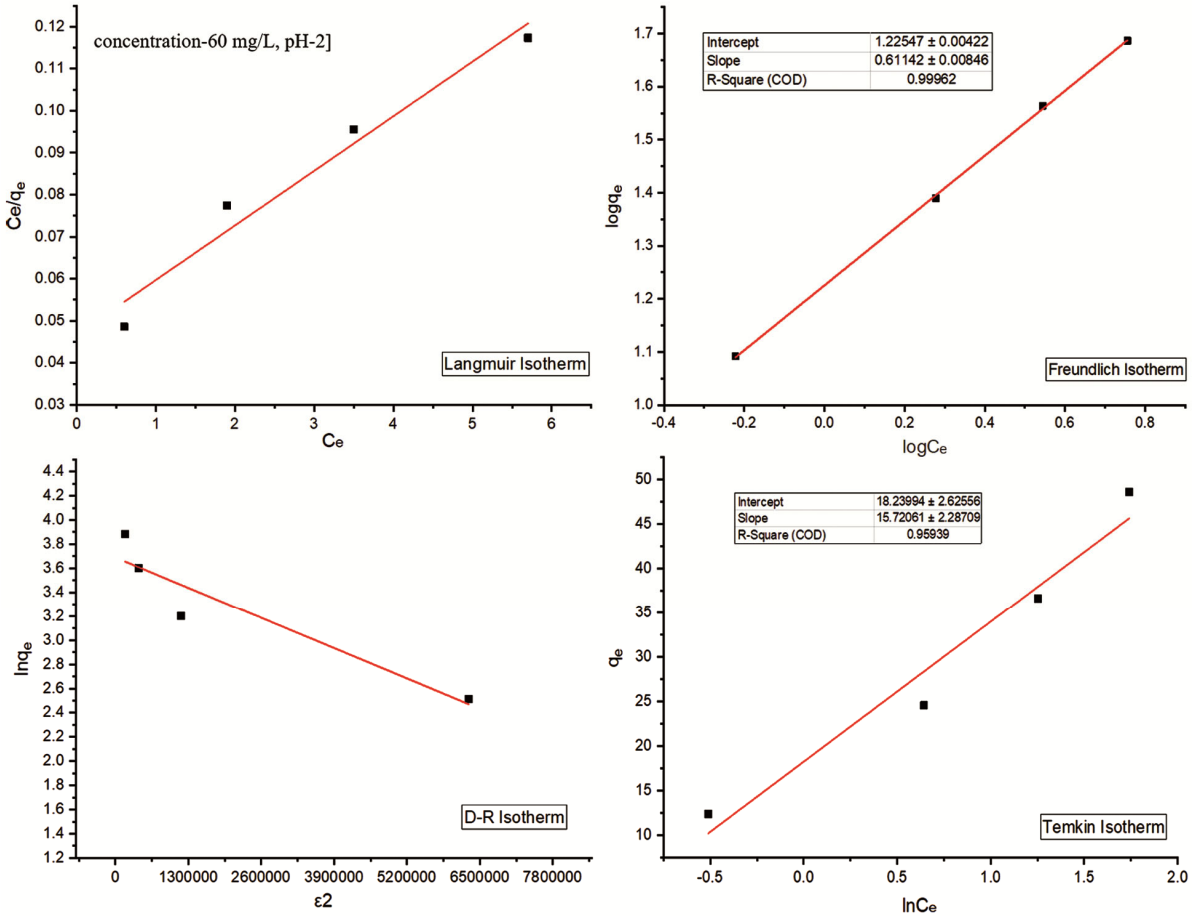

Fig. 6 — Plot of (a) Langmuir, (b) Freundlich, (c) Dubinin-Radushkevich, and (d) Temkin isotherms for the adsorption of CR onto carbon black

Table 2 — Kinetic model parameters

First-order kinetic model				Second-order kinetic model			
q_e(mg/g)	K_1 (1/min)	R^2	RMSE	q_e(mg/g)	K_2 (g/mg/min)	R^2	RMSE
3.80	0.0534	0.986	0.147	16.15	0.0058	0.998	0.141

affinities of the adsorption sites, making it more appropriate for surfaces with irregularities. Unlike the Langmuir isotherm, which assumes monolayer adsorption on a homogeneous surface, the Freundlich isotherm allows for multilayer adsorption. This characteristic makes it particularly useful when the adsorbate can form multiple layers on the surface, resulting in a higher adsorption capacity compared to the monolayer model of the Langmuir isotherm. Furthermore, the Freundlich isotherm models represent non-ideal adsorption behaviour, whereas the Langmuir isotherm assumes ideal adsorption conditions. If the adsorption process deviates from ideal behaviour, such as in the presence of surface heterogeneity or varying interactions between adsorbate molecules and surface sites, the Freundlich isotherm provides a more accurate representation of the adsorption process. Consequently, the Freundlich model is the preferred option to predict the adsorption capacity across a range of concentrations, particularly when dealing with complex adsorption systems.

The D-R isotherm parameter, mean free energy (E), helps to classify the adsorption process as either physisorption or chemisorption. Specifically, if E < 8(kJ/mol), the process is considered physisorption, while E > 16 (kJ/mol) indicates chemisorption[44,45]. In the current study, the observed value ofE was 0.508 (kJ/mol), which suggests that the adsorption process is predominantly physical in nature, with only minimal chemisorption occurring.

The Temkin model describes the indirect interactions between the adsorbate and the adsorbent. It assumes that the heat of adsorption decreases linearly as the surface coverage increases. In this study, the values of B_T and K_T were determined to be 162.806 (J/mol) and 3.190 (L/mg), respectively. The coefficient of determination (R^2) was calculated to be 0.959. Despite this, the Temkin isotherm model provided the least fit to the experimental data when compared to other models.

Adsorption kinetic models

The adsorption mechanism can be analyzed by fitting the batch adsorption data to various kinetic model equations. The pseudo-first-order and pseudo-second-order models are applied to evaluate the adsorption kinetics. The corresponding parameters for these kinetic models are provided in Table 2.

Pseudo-first-order model

According to this model, it is assumed that the adsorption of metal ions is directly proportional to the number of active sites available on the surface and can be expressed by Eq. (10) [46].

$$log(q_e - q_t) = log\, q_{e\,cal} - \frac{k_1}{2.030} t \quad \ldots (10)$$

Where k_1 represents the first-order rate constant (min^{-1}), q_e is the adsorbent uptake capacity at the equilibrium, and qt is the adsorbent uptake capacity at time *t*.

Utilizing the plot of ln(q_e - q_t) against time (t), the parameters k_1 and q_e can be determined. However, the correlation coefficients observed for the pseudo-first-order kinetic model were low, and notable disparities were evident between the experimental and theoretical parameters of equilibrium adsorption capacity (q_e). Consequently, it is indicated that the pseudo-first-order model inadequately fits the experimental statistics.

Pseudo-second-order model

In this model, the adsorption rate is assumed to be proportional to the square of the difference between the amount of adsorbate adsorbed at equilibrium and the amount of adsorbate adsorbed at time t[47]. This model's linear form is commonly expressed as given in Eq.(11).

$$\frac{t}{q_t} = \frac{1}{K_2 q_e^2} + \frac{t}{q_e} \quad \ldots (11)$$

Where the equilibrium rate constant for pseudo-second-order adsorption is denoted by K_2 (g/mg min).

By plotting t/q_t against time (t), a linear relationship is obtained (Fig. 7), and the slope and intercept of this line are utilized to compute the values of q_e and K_2.

The adsorption rate and mechanism of CR dye onto carbon black adsorbent were evaluated through non-linear regression analysis of both the pseudo-first-

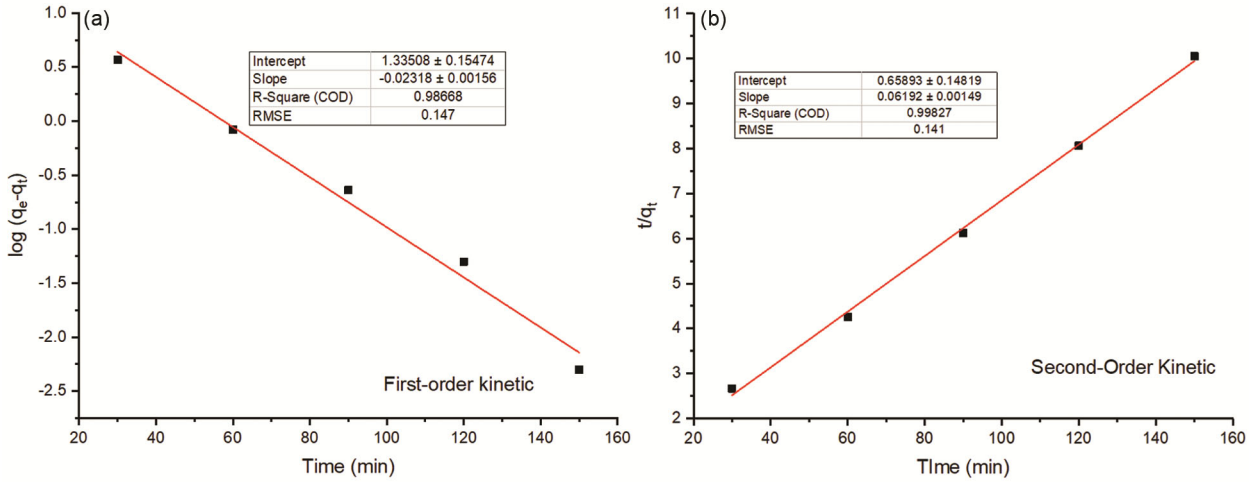

Fig. 7 — Kinetic plots for (a) pseudo-first order and (b) pseudo-second order for the adsorption of CR dye onto carbon black adsorbent

order and pseudo-second-order kinetic models, using the experimental data. The non-linear kinetic plots for the adsorption of CR ions onto the carbon black adsorbent are shown in Fig. 7. The calculated kinetic parameters are presented in Table 2.

Based on the higher R^2 value obtained, the pseudo-second-order kinetic model was found to provide a better fit for the adsorption process compared to the pseudo-first-order model. This suggests that the adsorption of CR ions onto the carbon black adsorbent predominantly follows a chemisorption mechanism, likely involving processes such as surface complexation and precipitation[48]. These processes are characteristic of chemical interactions between the adsorbate and the adsorbent surface, which involve the formation of chemical bonds. Despite the better fit of the pseudo-second-order model, the experimental equilibrium q_e values for CR ions were found to be closer to the theoretically calculated q_e values of the pseudo-first-order model. This indicates that, in addition to the chemisorption process, a physisorption mechanism[49], where adsorption occurs due to weaker electrostatic interactions between the adsorbate and the adsorbent, may also be present in the system[50]. The combination of both chemisorption and physisorption mechanisms highlights the complex nature of the adsorption method, suggesting that both chemical and physical interactions play significant roles in the overall adsorption of CR dye onto carbon black adsorbent.

Column adsorption studies

The continuous adsorption study was designed and analyzed using the Taguchi method, implemented through Minitab 18.0 software, to evaluate the performance of a column bed in removing CR dye from a liquid stream[31,51]. The primary performance metric used was the breakthrough time, which is the time required for the CR concentration in the effluent to reach 80% of its initial influent concentration. A longer breakthrough time signifies a more efficient adsorption process, indicating that the column bed can retain and remove CR from the liquid phase for an extended duration before the adsorbent's capacity is exceeded[52,53]. The study focused on three key operating parameters: flow rate (with levels of 2 mL/min, 4 mL/min, and 6 mL/min), bed diameter (1 cm, 2 cm, and 3 cm), and bed height (2 cm, 4 cm, and 6 cm). These parameters were varied systematically, with experimental runs conducted according to the combinations specified in Table 3**.** The analysis aimed to determine how each of these factors affects the breakthrough time, allowing for the identification of the optimal conditions under which

Table 3 — Experimental run according to Taguchi design and response (breakthrough time).

Flow Rate (mL/min)	Bed Height (cm)	Bed Diameter (cm)	Breakthrough Time (min)
2	2	1	64
2	4	2	85
2	6	3	108
4	2	2	48
4	4	3	59
4	6	1	61
6	2	3	36
6	4	1	39
6	6	2	51

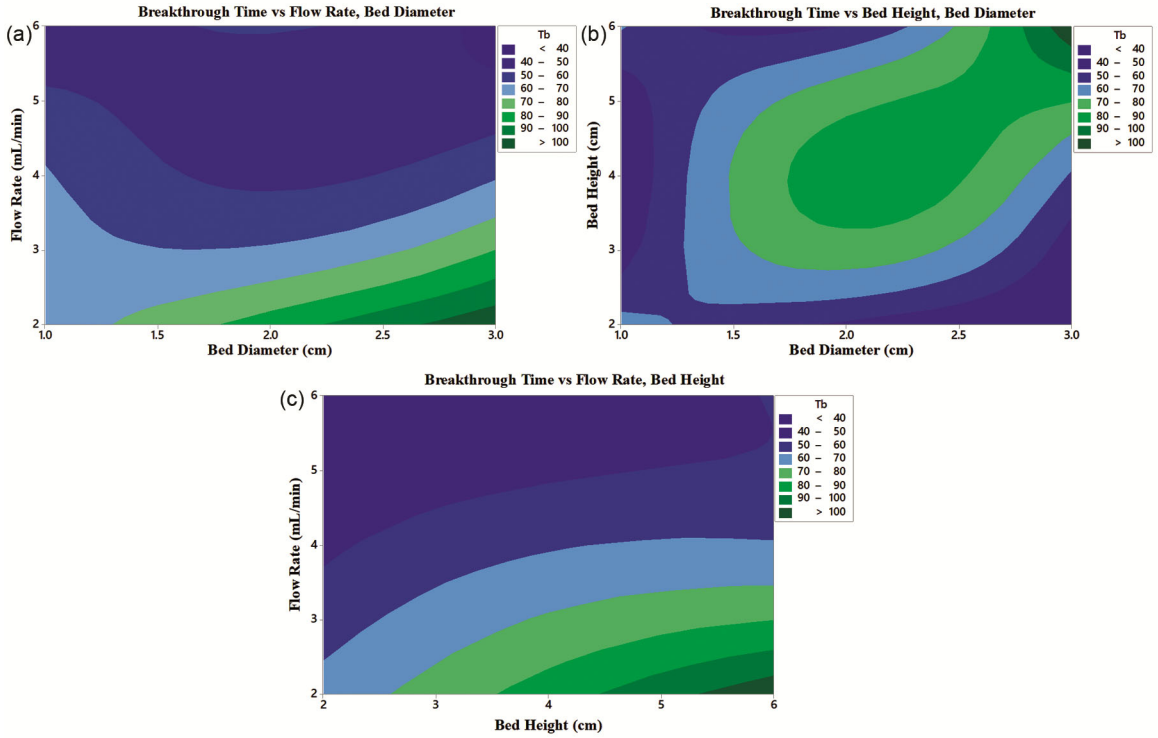

Fig. 8 — Simultaneous effect of parameters on breakthrough point: (a) bed diameter and flow rate, (b) bed diameter and flow rate and (c) bed height and flow rate

the adsorption process is most effective. Specifically, the flow rate influences the contact time between the liquid and the adsorbent, while bed diameter and bed height impact the available surface area and volume for adsorption, respectively. By examining the interplay of these parameters, the study provides a detailed understanding of how each factor contributes to the efficiency of the continuous adsorption system[54].

The simultaneous effect of two parameters on the breakthrough point is presented in the contour plot, as shown in Fig. 8. It can be observed that a low flow rate and large bed diameter are favourable for the large breakthrough time. This behaviour can be attributed to the fact that at higher flow rates, the residence time of the CR solution in the column is reduced, leading to a faster saturation of the adsorption sites. Additionally, the increased turbulence at higher flow rates contributes to a less efficient interaction between the CR dye molecules and the adsorbent surface and reduced intraparticle mass transfer, which hampers the adsorption process. It can be observed that a flow rate of less than 3 (mL/min) and abed diameter greater than 2 cm give more than 80% removal of CR dye. Similarly, a larger bed diameter provides a greater cross-sectional area for CR solution flow within the column. This increased cross-sectional area allows for a higher binding capacity of the adsorbent material, which results in a longer breakthrough time. The larger diameter reduces the velocity of the fluid across the adsorbent, enhancing the contact time between the adsorbate and the adsorbent, and thus improving the adsorption capacity.

From Fig. 8(b**)**, it can be observed that more than 90% removal of CR occurs when the bed height is larger than 5 cm and the bed diameter is larger than 2.7 cm. Large bed height increases the length of the adsorption zone, which provides more time for solute molecules to diffuse and interact with the adsorbent material. This results in a more efficient adsorption process, as the adsorbate molecules have more opportunities to be captured by the adsorbent. Fig. 8(c) suggested that a flow rate of less than 2.5 cm and a bed height of more than 4.5 cm had increased the removal of CR dye because of the increased adsorption zone and residence time. Table 4 presents the response table for the factors, which shows that the flow rate of CR dye through the bed is the most significant factor affecting the adsorption process.

Table 4 — Response Table for all the factors and their significance.

Level	Flow Rate (mL/min)	Bed Height (cm)	Bed Diameter (cm)
1	85.67	49.33	54.67
2	56.00	61.00	61.33
3	42.00	73.33	67.67
Delta	43.67	24.00	13.00
Rank	1	2	3

Conclusion

In this study, CR removal by adsorption onto carbon black was investigated. Characterization using SEM and FTIR revealed carbon black's homogeneous quasi-spherical morphology and the presence of oxygenated functional groups and hydrocarbons on its surface. Results showed that removal efficiency increased with time and adsorbent dose, while it decreased with increasing pH. The optimal conditions for maximum removal were determined to be pH 2, 60 min of contact time, and a 0.6 g/50mL adsorbent dose. The adsorption of CR ions onto carbon black adsorbents is best described by the Freundlich isotherm, indicating a heterogeneous surface with varying adsorption energies. The pseudo-second-order kinetic model provided a better fit than the Pseudo-first-order model, suggesting that the adsorption process predominantly follows a chemisorption mechanism, likely involving surface complexation and precipitation. These findings highlight that both physical and chemical interactions govern the adsorption process. From the continuous adsorption study, it was found that low flow rate, large bed height and bed diameter are favourable for the large breakthrough time. It was also found that the flow rate is the most significant parameter.

Acknowledgements

The authors are thankful to the Indian Institute of Technology Guwahati, Assam, India, and Guru Ghasidas Vishwavidyalaya Bilaspur, Chhattisgarh, India, for providing the research facilities.

Conflict of interest

The authors declare no conflict of interest.

References

1 Dhongde N R, Das N K, Banerjee T & Rajaraman P V, Synthesis of carbon quantum dots from rice husk for anti-corrosive coating applications: Experimental and theoretical investigations, *Ind Crops Prod*, 212 (2024) 118329.

2 Dhongde N R, Adhikari S & Rajaraman P V, Anticorrosion properties of ionic liquid functionalized graphene oxide epoxy composite coating on the carbon steel for CCUS environment, *Environ Sci Pollut Res*, 32 (2025) 4511.

3 Dhongde V, Velpandian M & Basu S, Exploring the impact of structural modification of double perovskite composite cathode material on oxygen reduction reaction in intermediate temperature solid oxide fuel cell, *Ionics*, 30 (2024) 8175.

4 Mohapatra T & Ghosh P, Degradation of eosin yellow dye solution by using nanosized copper based heterogenous fenton-like catalyst in a fluidised bed reactor, *Environ Degrad: Monit Assess Treat Technol*, (2022) 117.

5 Mohapatra T & Ghosh P, Fenton-like oxidation of eosin yellow using laterite catalyst in a circulating fluidized-bed reactor: Optimization, kinetics, and mass transfer study, *Chem Pap*, 77 (2023) 6285.

6 Mohapatra T, Manekar S, Kumar S V, Soni A K, Banerjee S & Ghosh P, Green synthesized Ag-TiO_2 for degradation of organic dye through visible light driven photo-reactor and its kinetics, *Int J Chem React Eng*, 19 (2021) 893.

7 Harja M, Buema G & Bucur D, Recent advances in removal of congo red dye by adsorption using an industrial waste, *Sci Rep*, 12 (2022) 6087.

8 Dutta A, Kundu D, Sharma S, Silvester D S & Banerjee T, Investigating the electrochemical properties of ionic-liquid-mediated inorganic eutectogels derived from carboxylic-acid-based hydrophobic natural deep eutectic solvents, *J Solution Chem*, 54 (2025) 1210.

9 Dutta A, Millar W, Silvester D S & Banerjee T, Novel eutectogels derived from an ionic-liquid-based deep eutectic solvent as electrolytes for supercapacitors: Synthesis and characterization, *New J Chem*, 48 (2024) 17787.

10 Dutta S, Gupta B, Srivastava S K & Gupta A K, Recent advances on the removal of dyes from wastewater using various adsorbents: A critical review, *Mater Adv*, 2 (2021) 4497.

11 Dutta A, Kundu D, Naik P K, Silvester D S & Banerjee T, Synthesis and properties of physically cross-linked silica-mediated novel eutectogels developed from carboxylic acid-based natural deep eutectic solvents, *Ind Eng Chem Res*, 63 (2024) 18390.

12 Dutta A, Kundu D, Sharma S, Paul N, Naik P K, Silvester D S & Banerjee T, Physically cross-linked titania-supported novel eutectogels as solid-state electrolytes: An experimental and quantum chemical investigation, *ACS Sustain Chem Eng*, 12 (2024) 248.

13 Litefti K, Freire M S, Stitou M & González-Álvarez J, Adsorption of an anionic dye (congo red) from aqueous solutions by pine bark, *Sci Rep*, 9 (2019) 16530.

14 Bai Z, Zheng Y & Zhang Z, One-pot synthesis of highly efficient MgO for the removal of congo red in aqueous solution, *J Mater Chem A Mater*, 5 (2017) 6630.

15 Jiang C, Yang C, Fu Y, Chen F & Hu J, High-efficiency Hg(II) adsorbent: Fes loaded on a carbon black from pyrolysis of waste tires and sequential reutilization as a photocatalyst, *Environ Sci Pollut Res*, 29 (56) 84287.

16 Han G, Du Y, Huang Y, Wang W, Su S & Liu B, Study on the removal of hazardous congo red from aqueous solutions by chelation flocculation and precipitation flotation process, *Chemosphere*, 289 (2022) 133109.

17 Al-Salihi S, Jasim A M, Fidalgo M M & Xing Y, Removal of congo red dyes from aqueous solutions by porous γ-alumina nanoshells, *Chemosphere*, 286 (2022) 131769.

18 Lal M K, Swain G, Kumar S R, Verma A & Sharan S R, Biodegradation of congo red dye using polyurethane foam-based biocarrier combined with activated carbon and sodium alginate: Batch and continuous study, *Bioresour Technol*, 351 (2022) 126999.

19 Meshram S, Thakur R S, Jyoti G, Thakur C & Soni A B, Optimization of lead adsorption from lead-acid battery recycling unit wastewater using H_2SO_4 modified activated carbon, *J Indian Chem Soc*, 99 (2022) 100469.

20 Dhongde V, Velpandian M, Haider M A & Basu S, A $Sr_2CoNbO_{6-\delta}$ @$Sm_{0.2}Ce_{0.8}O_{2-\delta}$ nanofiber composite as cathode accelerates oxygen reduction reaction for IT-SOFC, *ECS Trans*, 111 (2023) 2271.

21 Dhongde N R, Baranwal P K & Rajaraman P V, Functionalization of graphene oxide with an ionic liquid (1-butyl-3-methylimidazolium acetate): Preparation of epoxy-based coating on carbon steel for anticorrosive applications, *J Appl Polym Sci*, 140 (2023) e54026.

22 Adhikari S, Dhongde N R, Talukdar M K, Khan S & Rajaraman P V, Investigation of carbon steels (API 5L X52 and API 5L X60) dissolution CO_2–H_2S solutions in the presence of acetic acid: Mechanistic reaction pathway and kinetics, *Arab J Sci Eng*, 49 (2024) 8363.

23 Dhongde N R, Das N K, Hazarika J, Park J G, Banerjee T & Rajaraman P V, Azoles as corrosion inhibitors in alkaline medium for ruthenium chemical mechanical planarization applications: Electrochemical and theoretical analysis, *J Mol Struct*, 1320 (2025) 139651.

24 Trubetskaya A, Kling J, Ershag O, Attard T M & Schröder E, Removal of phenol and chlorine from wastewater using steam activated biomass soot and tire carbon black, *J Hazard Mater*, 365 (2019) 846.

25 Hamadi N, Adsorption kinetics for the removal of chromium(VI) from aqueous solution by adsorbents derived from used tyres and sawdust, *Chem Eng J*, 84 (2001) 95.

26 Wang J, Man H, Sun L & Zang S, Carbon black: A good adsorbent for triclosan removal from water, *Water*, 14 (2022) 576.

27 Jiang C, Yang C, Fu Y, Chen F & Hu J, High-efficiency Hg(II) adsorbent: FeS loaded on a carbon black from pyrolysis of waste tires and sequential reutilization as a photocatalyst, *Environ Sci Pollut Res*, 29 (2022) 84287.

28 El-Maadawy M M, Elzoghby A A, Masoud A M, Eldeeb A M, El-Naggar A M A & Taha M H, Conversion of carbon black recovered from waste tires into activated carbon *via* chemical/microwave methods for efficient removal of heavy metal ions from wastewater, *RSC Adv*, 14 (2024) 6324.

29 Liu W, Chen P, Sun Y, Huang C, Chen Y, Guo J, Pan J & Wan P, Converting pyrolysis carbon black derived from waste tires into a highly efficient adsorbent for dye wastewater treatment, *New J Chem*, 49 (2025) 11148.

30 Meshram S, Thakur C & Soni A B, Adsorption of Pb(II) form battery recycling unit effluent using granular activated carbon (GAC) and steam activated GAC, *Indian Chem Eng*, 63 (2021) 460.

31 Meshram S, Dharmadhikari S, Thakur R S, Soni A B & Thakur C, Fixed-bed adsorption of lead from battery recycling unit wastewater-optimization using Box-Behnken method, *J Hazard Mater Adv*, 10 (2023) 100297.

32 Sugatri R I, Wirasadewa Y C, Saputro K E, Muslih E Y, Ikono R & Nasir M, Recycled carbon black from waste of tire industry: Thermal study, *Microsyst Technol*, 24 (2018) 749.

33 Chen Y, Fan C, Li X, Ren J, Zhang G, Xie H, Liu B & Zhou G, Preparation of carbon black-based porous carbon adsorbents and study of toluene adsorption properties, *J Chem Technol Biotechnol*, 98 (2023) 117.

34 Dong P, Maneerung T, Ng W C, Zhen X, Dai Y, Tong Y W, Ting Y P, Koh S N, Wang C H & Neoh K G, Chemically treated carbon black waste and its potential applications, *J Hazard Mater*, 321 (2017) 62.

35 Fu Y, Liu X, Ge B & Liu Z, Role of chemical structures in coalbed methane adsorption for anthracites and bituminous coals, *Adsorption*, 23 (2017) 711.

36 Cardona-Uribe N, Betancur M & Martínez J D, Towards the chemical upgrading of the recovered carbon black derived from pyrolysis of end-of-life tires, *Sustain Mater Technol*, 28 (2021) e00287.

37 Wibawa P J, Nur M, Asy'ari M & Nur H, SEM, XRD and FTIR analyses of both ultrasonic and heat generated activated carbon black microstructures, *Heliyon*, 6 (2020) e03546.

38 El-Habacha M, Lagdali S, Dabagh A, Mahmoudy G, Assouani A, Benjelloun M, Miyah Y, Iaich S, Chiban M & Zerbet M, High efficiency of treated-phengite clay by sodium hydroxide for the congo red dye adsorption: Optimization, cost estimation, and mechanism study, *Environ Res*, 259 (2024) 119542.

39 Rose P K, Poonia V, Kumar R, Kataria N, Sharma P, Lamba J & Bhattacharya P, Congo red dye removal using modified banana leaves: Adsorption equilibrium, kinetics, and reusability analysis, *Groundw Sustain Dev*, 23 (2023) 101005.

40 Khan A, Naeem A, Mahmood T, Ahmad B, Ahmad Z, Farooq M & Saeed T, Mechanistic study on methyl orange and congo red adsorption onto polyvinyl pyrrolidone modified magnesium oxide, *Int J Environ Sci Technol*, 19 (2022) 2515.

41 Wang Y, Ren D, Ye J, Li Q, Yang D, Wu D, Zhao J & Zou Y, Highly efficient and targeted adsorption of congo red in a novel cationic copper-organic framework with three-dimensional cages, *Sep Purif Technol*, 329 (2024) 125149.

42 Alshammari R H, Aadil M, Kousar T, Maqbool U, Ahmad Z, Alswieleh A M, Algarni T S & Naeem M, Synthesis of binary metal doped CuO nanoarchitecture for congo red dye removal: Synergistic effects of adsorption and mineralization techniques, *Opt Mater*, 144 (2023) 114314.

43 El-Maadawy M M, Elzoghby A A, Masoud A M, Eldeeb A M, El-Naggar A M A & Taha M H, Conversion of carbon black recovered from waste tires into activated carbon *via* chemical/microwave methods for efficient removal of heavy metal ions from wastewater, *RSC Adv*, 14 (2024) 6324.

44 Konggidinata M I, Chao B, Lian Q, Subramaniam R, Zappi M & Gang D D, Equilibrium, kinetic and thermodynamic studies for adsorption of BTEX onto ordered mesoporous carbon (OMC), *J Hazard Mater*, 336 (2017) 249.

45 Sari A, Tuzen M, Citak D & Soylak M, Equilibrium, kinetic and thermodynamic studies of adsorption of Pb(II) from aqueous solution onto turkish kaolinite clay, *J Hazard Mater*, 149 (2007) 283.

46 Koujalagi P S, Divekar S V, Kulkarni R M & Cuerda-Correa E M, Sorption of hexavalent chromium from water and water-organic solvents onto an ion exchanger tulsion A-23(Gel), *Desal Water Treat*, 57 (2016) 23965.

47 Ho Y S & McKay G, Pseudo-second order model for sorption processes, *Process Biochem*, 34 (1999) 451.

48 Karaman C, Karaman O, Show P L, Karimi-Maleh H & Zare N, Congo red dye removal from aqueous environment by cationic surfactant modified-biomass derived carbon: Equilibrium, kinetic, and thermodynamic modeling, and forecasting via artificial neural network approach, *Chemosphere*, 290 (2022) 133346.

49 Yu K L, Lee X J, Ong H C, Chen W H, Chang J S, Lin C S, Show P L & Ling T C, Adsorptive removal of cationic methylene blue and anionic congo red dyes using wet-torrefied microalgal biochar: Equilibrium, kinetic and mechanism modelling, *Environ Pollut*, 272 (2021) 115986.

50 Sahar J, Naeem A, Farooq M, Zareen S & Farida S S, Kinetic studies of graphene oxide towards the removal of rhodamine B and congo red, *Int J Environ Anal Chem*, 101 (2021) 1258.

51 Amara-Rekkab A & Didi M A, Taguchi design for optimization of the removal of chromium(VI) by impregnated bentonite (K+) from aqueous solution, *Desal Water Treat*, 281 (2023) 186.

52 Xuan L N, Thi A T N & Thi M P D, Optimization and modeling of Pb^{2+} ions adsorption on bentonite and HNO_3-activated bentonite using taguchi and ANOVA methods, *Adsorpt Sci Technol*, 43 (2025) 1.

53 Marimuthu S, Mani M G V, Ganapathiappan R & Rajendran K, Statistical optimization and characterization of fluoride biosorption using dead microbial biomass *Indian J Chem Technol*, 31 (2024) 494.

54 Bambal A, Jugade R, Sarvanan D & Pakade Y, Sequestration of Ni(II) ions from water bodies by using gamma-sterilized biowaste, *Indian J Chem Technol*, 31 (2024) 738.